Reaction between NO and CO on Rh(100): how lateral interactions lead to auto-accelerating kinetics

Please check the document version of this publication:

Reaction between NO and CO on rhodium (100): How lateral interactions lead to auto-accelerating kinetics

M. J. P. Hopstaken and J. W. Niemantsverdriet[a]
Schuit Institute of Catalysis, Eindhoven University of Technology, 5600 MB Eindhoven, The Netherlands

The reactions between NO and CO adsorbed on Rh(100) were studied with temperature programmed reaction spectrometry and static secondary ion mass spectrometry and compared with similar reactions on Rh(111). Elementary steps in the overall reactions, such as dissociation of NO, and reaction between CO and O atoms were studied as well. Dissociation of NO is faster on the more open Rh(100) surface, while formation of N_2 is slower. Desorption of either CO or NO occurs at comparable rates on Rh(100) and Rh(111). The oxidation of CO to CO_2 proceeds much faster on Rh(100) than on Rh(111). When the Rh(100) surface is saturated with NO and CO, explosive formation of CO_2 is observed, which can be explained by an autocatalytic mechanism, in which the availability of empty sites plays a crucial role. © *2000 American Vacuum Society.* [S0734-2101(00)01704-8]

I. INTRODUCTION

The reaction between CO and NO on rhodium is of great practical interest for the removal of NO_x from automotive exhaust.[1] The reaction has been studied extensively on the densely packed Rh(111) surface, as reviewed recently by Zhdanov and Kasemo.[2] Kinetic parameters for all elementary steps in the CO+NO reaction on Rh(111) have been determined, be it at low coverages of the participating molecules.[2,3]

Much less is known about the CO + NO reaction on Rh(100). The overall kinetics reported by Peden *et al.*[4] indicate that the effective activation energy for the reaction on Rh(100) is lower than on Rh(111). In this article we use temperature programmed reaction spectroscopy and static secondary ion mass spectrometry to investigate the reaction between preadsorbed CO and NO, and relevant elementary surface reactions such as the dissociation of NO and the reaction between O atoms and CO on the Rh(100) surface. Comparison with results obtained for Rh(111) shows that the Rh(100) surface is not only more active for dissociation of NO—as expected—but also significantly more active and selective for the subsequent oxidation of CO by oxygen atoms. Recombination of N atoms, on the other hand, proceeds much slower on Rh(100) than on Rh(111).

II. EXPERIMENT

Experiments were done in an ultrahigh vacuum (UHV) stainless-steel chamber (base pressure $<1\times10^{-10}$ mbar) equipped with Auger electron spectroscopy (AES) (Leybold AE10), temperature programmed reaction spectroscopy (TPRS), and temperature programmed static secondary ion mass spectrometry (TPSSIMS) (Leybold SSM200), previously described elsewhere.[5] The Rh(100) crystal was mounted on tantalum wires and could be cooled down with

[a]Author to whom correspondence should be addressed; electronic mail: J.W.Niemantsverdriet@tue.nl

liquid nitrogen to 100 K and resistively heated to 1425 K. A temperature controller (Eurotherm) allowed for a constant heating rate in temperature programming. The crystal surface was cleaned by cycles of argon sputtering and annealing under oxygen and UHV, as previously described.[6] Crystal cleanliness was verified by AES, static secondary ion mass spectroscopy (SSIMS), and by the absence of CO and CO_2 in temperature programmed deposition (TPD) after O_2 adsorption.

III. RESULTS AND DISCUSSION

A. Reaction of NO+CO on Rh(100) and Rh(111)

Figure 1 shows the temperature programmed reaction between NO and CO on both the (111) and the (100) surfaces of rhodium, representing typical cases of the reaction at low coverage where CO_2, N_2, and CO are the only desorbing products.

On Rh(111) (left panel) we have used isotopically labeled ^{13}CO to discriminate between N_2 and CO, and CO_2 and N_2O. The latter product is not observed, however, under UHV conditions. Obviously, dissociation of NO is complete at these low coverages as evidenced by the absence of NO in the TPD spectra and the formation of N_2 in the temperature range from 500 to 700 K. Production of CO_2 is observed around 450 K. Note that CO and CO_2 desorb in the same temperature range, indicating that CO desorption competes with CO_2 formation on Rh(111). The selectivity to CO_2 is low, in this case only 30% of the initially adsorbed CO reacts with O to form CO_2.

A similar experiment with comparable starting coverages of CO and NO on Rh(100) gives considerably different results, as the right panel of Fig. 1 shows. As desorption of CO and formation of N_2 are well separated in temperature (as confirmed by the cracking patterns at 12 and 14 amu), there is no need for using labeled CO. First, CO_2 production starts already at 300 K, which is much lower than on Rh(111).
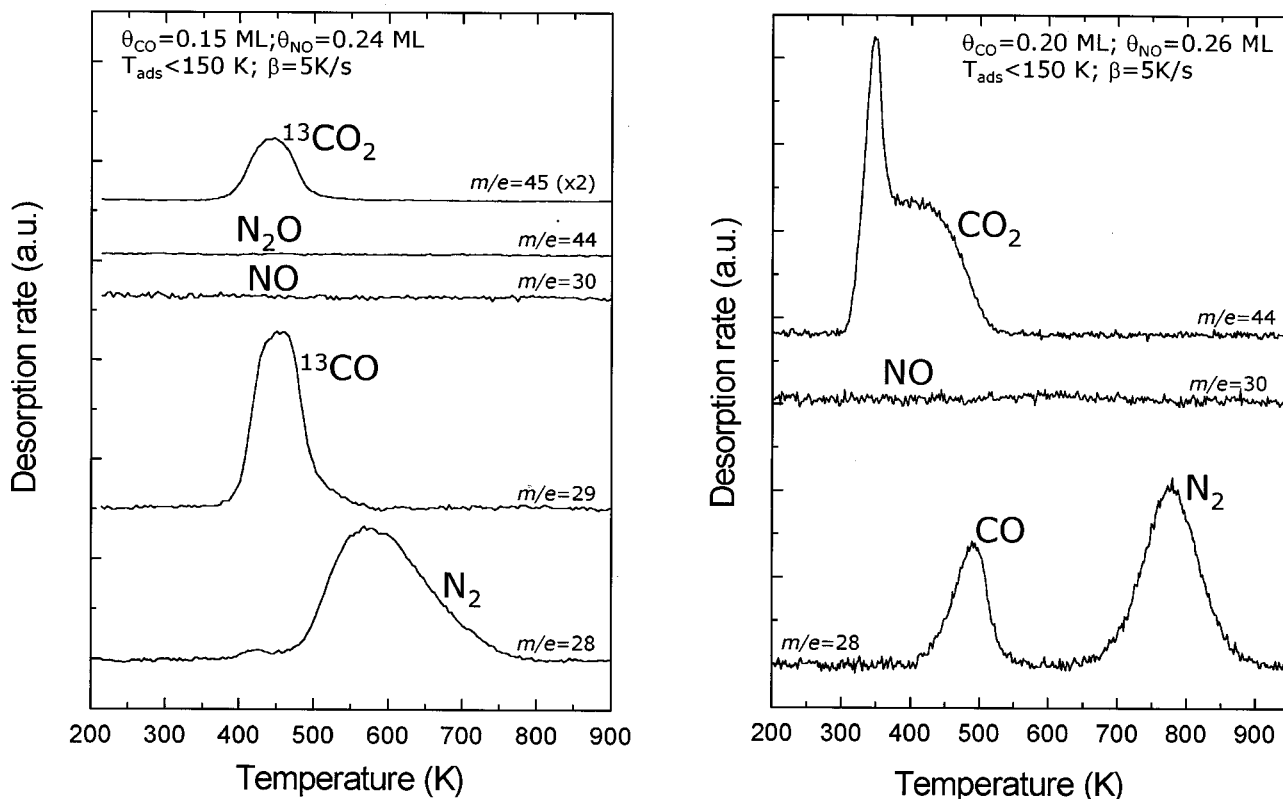
FIG. 1. Temperature programmed reactions of 0.15 ML of ^{13}CO coadsorbed with 0.24 ML of NO on Rh(111) (left panel) and 0.20 ML of CO coadsorbed with 0.26 ML NO on Rh(100) (right panel). Reactants were adsorbed at 150 K; the heating rate was 5 K/s.

Also, most of the CO_2 forms before CO starts to desorb, hence, the two processes do not compete as on Rh(111). With oxidation of CO favored over desorption, the selectivity to CO_2 corresponds to about 80% of the initially adsorbed CO, whereas it is only 30% on Rh(111). Second, formation of N_2 is considerably slower than on Rh(111), as the TPD peak between 700 and 850 K indicates. This is as expected, as atomic adsorbates bind more strongly on the more open surfaces.[7]

TPRS reveals the kinetics of surface reactions only if these result in the instantaneous desorption of the product, as is the case with CO_2 and N_2 formation. For the NO decomposition step, however, the dissociation products remain on the surface and react to desorbing products at higher temperatures. Hence, to monitor this step we need a technique able to monitor changes in coverages of adsorbed species. To this end we use SIMS.

B. Dissociation and desorption of NO on Rh(100)

As explained elsewhere,[8,9] the presence of adsorbed species such as NO, N, and O is best reflected by secondary ions of the type Rh_2NO^+, Rh_2N^+, and Rh_2O^+. Provided coverages are not too high, quantitation is usually achieved by correlating intensity ratios such as Rh_2NO^+/Rh_2^+ and Rh_2N^+/Rh_2^+ with the coverages of the corresponding species, respectively.

Figure 2 shows TPD and TPSSIMS intensity ratios, illustrative for NO desorption and dissociation of NO in three

different coverage regimes: low ($\theta_{NO} < 0.28$ ML), intermediate ($0.28 < \theta_{NO} < \sim 0.50$ ML), and high ($\theta_{NO} > 0.50$ ML).

1. $\theta_{NO} < 0.28$ ML

The low coverage range is characterized by complete NO dissociation. For the lowest coverages, dissociation starts around 170 K and is completed around 250 K. With increasing coverage, the onset of dissociation shifts slightly to about 200 K. However, the completion of dissociation is significantly more retarded to 375 K. Hence, dissociation is hindered due to interaction of the dissociating NO molecule with other NO molecules (shift in onset of dissociation from 170 to 200 K), and with its dissociation products, N_{ads} and O_{ads}, which retard the dissociation up to 375 K. Hence, the adsorbed atoms appear to affect the dissociation of NO most. N atoms recombine around 750 K, as evidenced by the desorption of N_2 and the concomittant decrease in the Rh_2N^+/Rh_2^+ ion intensity ratio. Using leading edge and Chan–Aris–Weinberg analysis, we find an activation barrier 215 ± 10 kJ/mole and a preexponential factor $10^{15.1 \pm 1}$ s^{-1} for N_2 formation on Rh(100).

2. $0.28 < \theta_{NO} < \sim 0.50$ ML

In the medium coverage range, NO dissociates until all sites are occupied, after which the remaining NO starts to desorb when the temperature reaches about 400 K. Additional NO dissociates on the empty sites freed by desorption
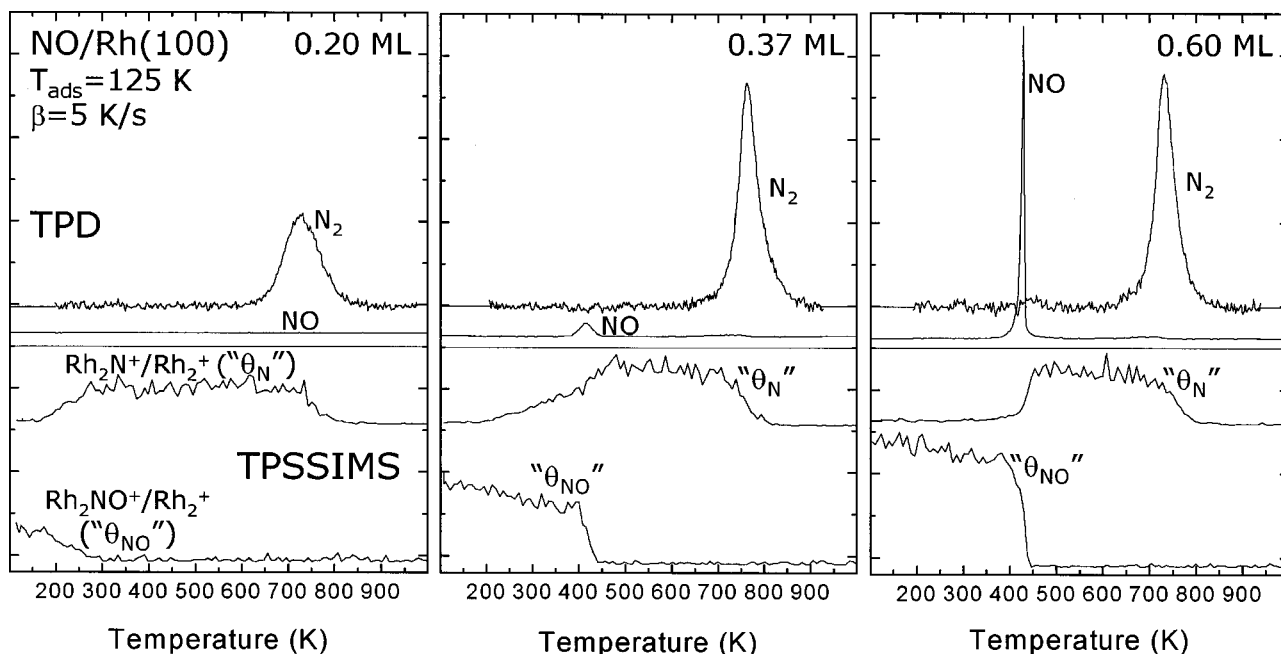
FIG. 2. Selected NO and N_2 desorption rates (top), and $Rh_2(NO)^+/Rh_2^+$ and Rh_2N^+/Rh_2^+ TPSSIMS ion intensity ratios, representing the surface coverages of NO and N atoms respectively, (bottom), during temperature programmed reaction of NO on Rh(100), for low (left), medium (central), and high (right) initial NO coverages.

of NO, due to the creation of vacancies in the relatively small temperature regime between 400 and 430 K. The effect is best seen in the increase in the SIMS intensity ratio characteristic of atomic nitrogen, Rh_2N^+/Rh_2^+, since the decrease in the corresponding signal for NO reflects both desorption and dissociation. Note that the desorbing NO molecules do so from an environment containing atomic and molecular species. Using Redhead analysis, we estimate an activation barrier of 106 ± 10 kJ/mole for NO desorption, assuming a preexponential factor of $10^{13.5}$ s^{-1}. Note, however, that the NO desorption kinetics is clearly influenced by the presence of coadsorbed atomic species.

3. ~0.50 ML < $\theta_{NO} \leqslant 0.65$ ML

At coverages close to saturation, dissociation is self-inhibited until desorption of NO takes place at temperatures above 400 K. Here desorption and dissociation of NO occur rapidly in a narrow temperature region. The onset of NO desorption is delayed by ~25 K (from ~375 K at 0.40 ML to ~400 K at 0.60 ML), which we attribute to the absence of atomic species and the associated repulsive N–NO and O–NO interactions. Note that at the onset of the desorption, at 400 K, NO molecules leave from an environment of NO molecules. As discussed earlier, desorption of NO from a mixed environment of atomic and molecular species starts at 375 K already. Apparently, repulsion between NO molecules is smaller than repulsion between NO and its dissociation products. The remarkably sharp shape of the NO desorption peak and the steep increase in the SIMS signal for atomic nitrogen in Fig. 2 can now be explained by an autocatalytic mechanism and the delicate interplay of repulsive interactions: as soon as the first NO molecules desorb, empty sites

become available for dissociation. Since dissociation of NO is a very rapid process at this temperature, these empty sites are filled instantaneously by N_{ads} and O_{ads}. These atoms enhance the NO desorption rate, and more empty sites become available. This mechanism results in an explosive increase in the rates for both desorption and dissociation until all NO has disappeared from the surface.

Hence, the rate of NO dissociation on Rh(100) is strongly affected by several factors, such as the availability of vacant sites and lateral interactions between the dissociating molecule and coadsorbed NO, N, and O. We have therefore determined the kinetic parameters for the dissociation step in the limit of zero coverage. Assuming a preexponential factor of 10^{11} s^{-1}, in line with theory predictions by van Daelen et al.[10] for NO on Cu clusters, we find an activation energy E_{dis} of 37 ± 3 kJ/mole. This is in good agreement with the 34 kJ/mole predicted by Shustorovich and Bell,[11] using bond-order conservation Morse potential calculations. For NO coverages up to 0.30 ML, the dissociation kinetics on Rh(100) can be modeled by a combination of site blocking and lateral interactions. Site blocking is modeled by assuming that NO needs at least one free neighboring site in order to dissociate and lateral interactions are accounted for by assuming that E_{dis} increases stronger than linear with total adsorbate coverage. This is extensively described in Ref. 6. The value of 44 ± 3 kJ/mole reported by Villarubia and Ho,[12] valid at a NO coverage of 0.15 ML, agrees very well with our value derived for the same coverage.

The decomposition and desorption of NO on Rh(100) shows many similarities with the same reactions on the more densely packed Rh(111) surface.[5,6,12–15] On both surfaces, NO adsorbs molecularly at low temperatures, and upon heat-

TABLE I. Kinetic parameters for the elementary reaction steps involved in the CO+NO reaction on Rh(100) and Rh(111).

Elementary reaction	E_{act} (kJ/mole)	ν (s^{-1})	E_{act} (kJ/mole)	ν (s^{-1})	Remarks
	Rh (111)		Rh(100)		
$NO_{ads}+* \rightarrow N_{ads} + O_{ads}$	65 ± 6	$10^{11\pm1.0}$	37 ± 3	$10^{11\pm1.0}$	Low coverage limit[a]
$NO_{ads}\rightarrow NO_{gas}+*$	113 ± 10	$10^{13.5\pm1.0}$	106 ± 10	$10^{13.5\pm1.0}$	At $\theta_N=\theta_O=0.25$ ML for Rh(111) 0.28 ML for Rh(100)[a]
$N_{ads}+N_{ads}\rightarrow N_2+2*$	118 ± 10	$10^{10\pm1.0}$	215 ± 10	$10^{15.1\pm0.5}$	Low coverage limit[a]
$CO_{ads}+O_{ads}\rightarrow CO_2+2*$	67 ± 3	$10^{7.3\pm0.2}$	90 ± 7	$10^{11.2\pm0.7}$	Rh(111): $\theta_O=0.17$ ML; $\theta_{CO}\rightarrow0$[b] Rh(100): $\theta_O=0.16$ ML; $\theta_{CO}\rightarrow0$[c]
$CO_{ads}\rightarrow CO_{gas}+*$	159 ± 5	$10^{15\pm1.0}$	140 ± 2	$10^{14.4\pm0.2}$	Low coverage limit[c]

[a]See Refs. 5 and 6.
[b]See Ref. 3.
[c]See Ref. 13.

ing the NO at small coverages ($\theta_{NO}<0.25$ ML), dissociation to N_{ads} and O_{ads} is complete. On both surfaces, nitrogen atoms exclusively recombine to form N_2 and formation of N_2O is not observed under UHV conditions. The activation energies for dissociation of NO and desorption of N_2, however, differ substantially, see Table I.

Apparently, the more open Rh(100) surface is intrinsically more active in the dissociation of NO than the densely packed Rh(111) surface. On the other hand, nitrogen formation on Rh(100) is considerably slower than on Rh(111). This can be explained by the stronger bonding of atomic adsorbates on more open surfaces,[7] which makes dissociation more easy but slows down the recombination of N atoms to form N_2.

C. Oxidation of CO on Rh(100)

CO oxidation provides the pathway in which O atoms are removed from the rhodium surface, since O atoms only recombine to form O_2 at elevated temperatures (>1000 K). Figure 3 gives an overview of the temperature-programmed reaction between a fixed amount of preadsorbed oxygen ($\theta_O=0.16$ ML), deposited by exposing the crystal to an O_2/Ar mixture (20%/80%) at 273 K, and different amounts of CO, adsorbed below 175 K. Integration of the CO_2 and CO TPD spectra (panel A) yields the fraction of reacted and desorbed CO as a function of initial CO coverage (panel B). Application of coverage-corrected leading edge analysis[3] to the low-coverage CO_2 TPD spectra yields kinetic parameters (panel C). Similar experiments as in Fig. 3 were done for different amounts of precovered oxygen. In all cases desorption of CO is observed only when all oxygen atoms have reacted to CO_2. In the experiment of Fig. 3, CO_2 starts to form in a single state around 430 K. Leading edge analysis yields an activation energy of 90 ± 7 kJ/mole and a preexponential factor of $10^{11.2\pm0.7}$ s^{-1} in the limit of zero coverage. The activation energy for CO oxidation appears to decrease with increasing CO coverage. This is, however, compensated by a corresponding decrease in the pre-exponential factor. At higher CO coverages (i.e., $\theta_{CO}>0.2$ ML), an additional, fast channel for CO_2 formation opens up, as evidenced by a shoulder around 350 K, which grows into a peak around 270 K. As stated before, reaction between CO and O to CO_2 is complete as long as oxygen is present in excess, as shown in panel B.

The kinetics of CO oxidation depend strongly on CO and O coverage, where higher coverages accelerate the rate.

The most striking difference in CO oxidation kinetics on Rh(100) and Rh(111) is that oxidation is faster on the (100) surface, as evident from Fig. 1. Table I summarizes the kinetic parameters for all relevant elementary steps on both Rh(100) and Rh(111) as obtained in this and previous work.

D. Explosive formation of CO_2 on Rh(100)

We have examined the reaction between CO and NO over a broad range of reactant coverages on both Rh(111)[3] and Rh(100). A special case arises when the Rh(100) surface is saturated with an overlayer of CO and NO, since the site requirement of the NO dissociation step delays all chemistry until desorption of one of the reactants liberates sites on the surface. We have investigated this case with SIMS and TPD.

Figure 4 shows the desorption rates and characteristic SIMS intensity ratios during temperature programming of 0.20 ML CO coadsorbed with 0.60 ML NO on Rh(100). Up to a temperature of 300 K no reaction takes place, as evident from the absence of any desorbing species and the fact that all adsorbate coverages are constant. Around 350 K a small amount of CO desorbs, freeing up some empty sites. This triggers all further surface reactions: at 350 K dissociation of NO starts as evidenced by the increase in the Rh_2N^+/Rh_2^+ ion intensity ratio. Note that at these high coverages the SIMS intensity ratios are at best a qualitative indicator of coverage. The Rh_2O^+/Rh_2^+ ratio also increases slightly, but less than when the same amount of NO is adsorbed on Rh(100) alone since O atoms are now rapidly consumed by CO. This results in a very sharp CO_2 peak which maximizes around 395 K. As all CO has been consumed at 400 K, see the Rh_2CO^+/Rh_2^+ ion intensity ratio, CO_2 production ends abruptly. This 'explosive' CO_2 formation has also been observed on Pt(100),[16] Pd(320),[17] and Pd(100)[18] and can be explained by the following mechanism:
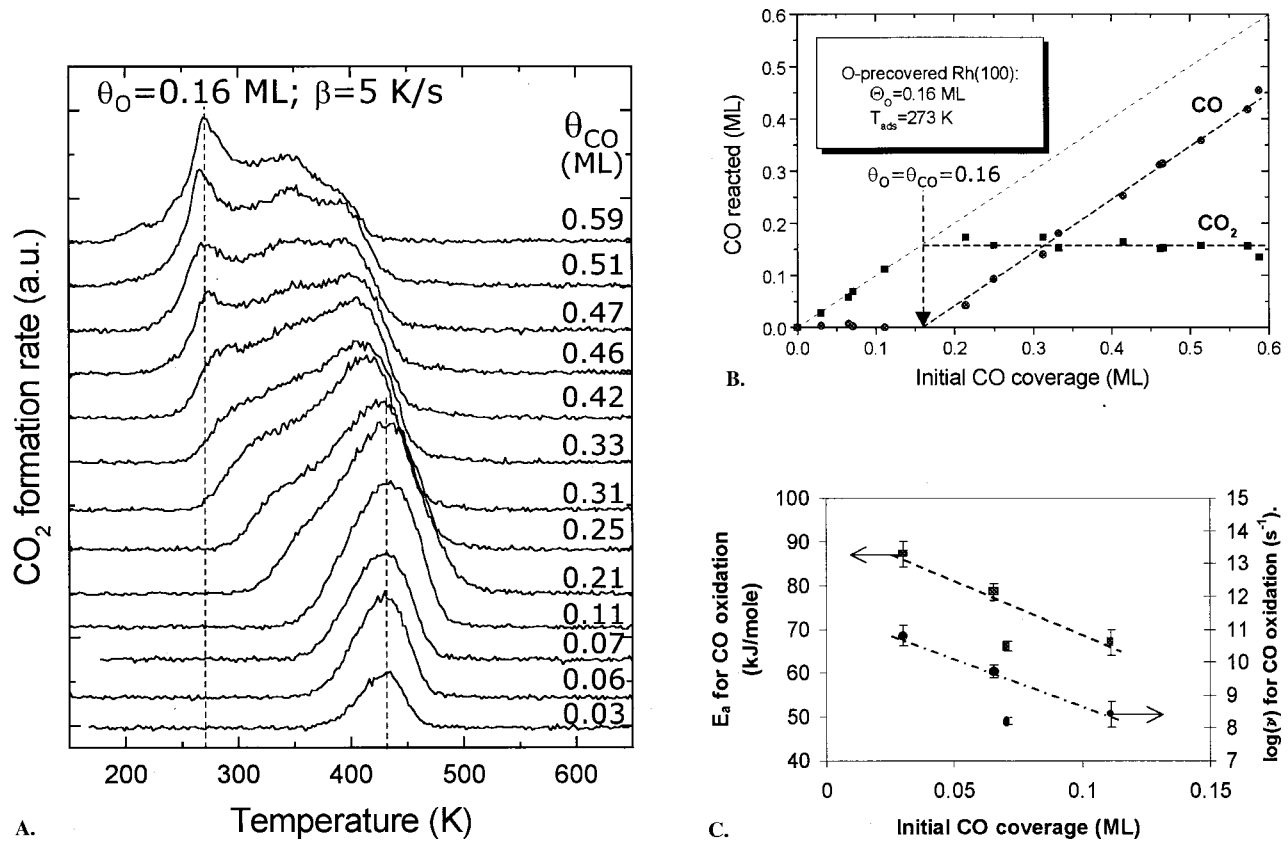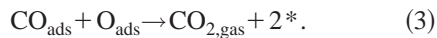
FIG. 3. CO_2 formation from different amounts of CO on Rh(100) precovered by 0.16 ML of O atoms ($T_{ads}=273$ K), along with the amounts of CO which have desorbed and reacted with O to form CO_2 as derived from the CO and CO_2 TPD peak areas (B), and kinetic parameters as a function of initial CO coverage, derived by coverage-corrected leading edge analysis (C).

Reaction trigger: $CO_{ads} \rightarrow CO_{gas} + {}^*$,   (1)

$$NO + {}^* \rightarrow N_{ads} + O_{ads},   (2)$$

$$CO_{ads} + O_{ads} \rightarrow CO_{2,gas} + 2{}^*.   (3)$$

Provided the adsorbed molecules have sufficient mobility over the surface, reactions (2) and (3) are autocatalytic in the free sites: dissociation of NO [reaction (2)] requires one empty site but the subsequent formation of CO_2 liberates two sites, the overall reaction being $CO_{ads} + NO_{ads} + {}^* \rightarrow CO_{2,gas} + N_{ads} + 2{}^*$, emphasizing the autocatalytic nature. But the effect is even stronger than caused by generation of empty sites alone. As we have shown for NO on Rh(100), the dissociation is retarded at higher coverages, especially by the presence of N_{ads} and O_{ads}, so the removal of oxygen by CO relieves the retarding effect of atomic adsorbates on the dissociation somewhat.

As all CO has been consumed at 400 K, CO_2 production stops abruptly and some excess NO desorbs between 400 and 450 K. In this temperature range, additional NO is dissociated, as evidenced by the increase in the Rh_2N^+/Rh_2^+ and Rh_2O^+/Rh_2^+ ion intensity ratio. The decrease in the Rh_2NO^+/Rh_2^+ ratio reflects the decrease in θ_{NO}, both by desorption and dissociation.

Up to 700 K, N and O coverages stay constant. Between 700 and 850 K, N atoms recombine to form N_2 as evidenced by TPD and the concomittant decrease in the Rh_2N^+/Rh_2^+ ratio. From the NO and N_2 TPD peak areas, we derive that about 85% of the amount of initially adsorbed NO has dissociated. This is considerably higher than in the case when 0.60 ML NO is adsorbed without CO, where only 55% of the NO decomposes.[6] Hence, coadsorbed CO offers a reaction channel to remove O atoms as CO_2, enabling NO to dissociate to a higher extent.

IV. CONCLUSIONS

(1) Dissociation of NO is intrinsically faster on the more open Rh(100) than on Rh(111), due to the higher heat of adsorption of the decomposition products on the former. This, on the other hand, slows down the formation of N_2. Desorption of molecular NO proceeds with similar kinetic parameters on Rh(111) and Rh(100), see Table I.

(2) Dissociation of NO on Rh(100) is progressively retarded at higher coverages, both by site blocking and by lateral interactions with coadsorbed species, which increase the activation barrier E_{dis} for dissociation. The dissociation kinetics of NO on Rh(100) can be satisfactorily described by
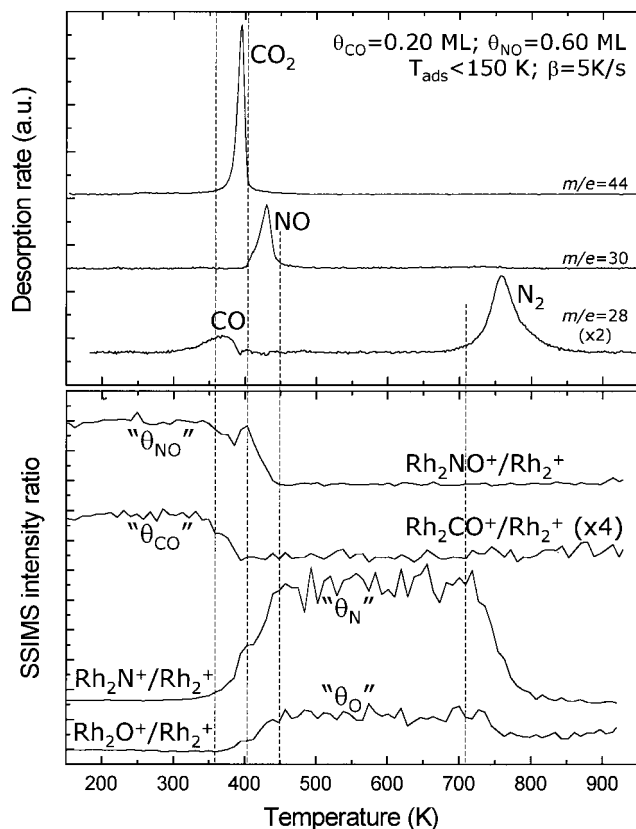
FIG. 4. Desorption of products and SIMS intensity ratios during temperature programmed reaction of 0.20 ML of CO coadsorbed with 0.60 ML of NO on Rh(100). Reactants were adsorbed at 150 K and the applied heating rate was 5 K/s in both experiments.

assuming that a NO molecule requires only one free Rh site and that E_{dis} increases stronger than linear with total coverage. The latter emphasizes that repulsive lateral interactions only come into play at higher coverages.

(3) Oxidation of CO is more effective on Rh(100) than on Rh(111). On Rh(111) desorption competes strongly with oxidation of CO, whereas on Rh(100) the CO oxidizes stoichiometrically with all available O atoms.

(4) Temperature programming of CO and NO coadsorbed on Rh(100) at saturation coverage, leads to explosive formation of CO_2 in an autocatalytic mechanism which is triggered by the desorption of CO.

[1] K. C. Taylor, Catal. Rev. Sci. Eng. **35**, 457 (1993).
[2] V. P. Zhdanov and B. Kasemo, Surf. Sci. Rep. **29**, 31 (1997), and references therein.
[3] M. J. P. Hopstaken, W. J. H. van Gennip, and J. W. Niemantsverdriet, Surf. Sci. **433−435**, 69 (1999).
[4] C. H. F. Peden, D. W. Goodman, D. S. Blair, P. J. Berlowitz, G. B. Fisher, and S. H. Oh, J. Phys. Chem. **92**, 1563 (1988).
[5] H. J. Borg, J. P. C.-J. M. Reijerse, R. A. van Santen, and J. W. Niemantsverdriet, J. Phys. Chem. **101**, 10052 (1994).
[6] M. J. P. Hopstaken and J. W. Niemantsverdriet, J. Phys. Chem. B (to be published).
[7] R. A. van Santen and J. W. Niemantsverdriet, *Chemical Kinetics and Catalysis* (Plenum, New York, 1995).
[8] A. Brown and J. C. Vickerman, Surf. Sci. **124**, 267 (1983).
[9] H. J. Borg and J. W. Niemantsverdriet, in *Catalysis*, A Specialist Periodical Report, edited by J. J. Spivey and A. K. Agarwal (The Royal Society of Chemistry, Cambridge, 1994), Vol. 11, p. 1.
[10] M. A. van Daelen, Y. S. Li, J. M. Newsam, and R. A. van Santen, J. Phys. Chem. **100**, 2279 (1996).
[11] E. Shustorovich and A. T. Bell, Surf. Sci. **289**, 127 (1993).
[12] J. S. Villarubia and W. Ho, J. Chem. Phys. **87**, 750 (1987).
[13] P. Ho and J. M. White, Surf. Sci. **137**, 103 (1984).
[14] T. W. Root, L. D. Schmidt, and G. B. Fisher, Surf. Sci. **134**, 30 (1983).
[15] T. W. Root, G. B. Fisher, and L. D. Schmidt, J. Chem. Phys. **85**, 4679 (1986).
[16] M. W. Lesley and L. D. Schmidt, Surf. Sci. **155**, 215 (1985).
[17] M. Hirsimäki, S. Suhonen, J. Pere, M. Valden, and M. Pessa, Surf. Sci. **402−404**, 187 (1998).
[18] M. Daté, H. Okuyama, N. Tagaki, M. Nishijima, and T. Aruga, Surf. Sci. **350**, 79 (1996).